Spiral Servo Writing in Hard Disk Drives Using Iterative Learning Based Tracking Control

Xu Chen * **and Masayoshi Tomizuka** *

* *Department of Mechanical Engineering, University of California, Berkeley, CA, 94720, USA (e-mails: {maxchen,tomizuka}@me.berkeley.edu).*

Abstract: The servo control in a hard disk drive (HDD) system relies heavily on the position information obtained from the servo sectors. As the tracks-per-inch (TPI) gets higher and higher in HDDs, writing of servo sectors takes a longer and longer time. One way to solve this problem is to use servo track writers to write spiral servo patterns on the disks and then perform self servo writing (SSW) within each HDD unit. The quality of the spirals is the key to achieve high TPI in SSW. This paper discusses high precision tracking control algorithms for the writing of spiral servo patterns. An iterative learning scheme is introduced, which combines a disturbance observer with the zero phase error tracking algorithm, and develops a new way of designing asymptotically optimal feedforward inputs for a general two degree of freedom control systems. In learning control schemes, non-repetitive disturbances have an adverse influence on the tracking performance. The paper analyzes this situation, and develops a robust learning scheme to deal with the problem.

Keywords: digital control, learning control, tracking control, data storage devices

1. INTRODUCTION

In modern hard disk drives (HDDs), servo sectors (a.k.a. servo wedges) provide the position information for the read/write heads to access the user data. These specially coded magnetic patterns are pre-written in the factory, at fixed intervals on every data track in the HDD, as demonstrated in Fig. 1a. There are tens of millions of servo sectors on a single disk platter (Al Mamun et al. (2007)). This number is nowadays still rapidly increasing, as the HDD manufactures continuously extend their product storage capacities.

Writing of the servo sectors used to be performed entirely on devices called servo track writers. As the area density gets higher and higher, writing of the servo sectors takes a longer and longer time. One way to reduce the servo writing cost is to let HDDs write the servo sectors themselves, provided that some additional reference patterns are given. This introduced the so-called spiral based servo writing technique (see, e.g., Vinay K. Agarwal (2006) and Mizukoshi et al. (2010)), where the additional reference patterns are named spiral servo patterns as demonstrated in Fig. 1b. These spiral patterns are first written on the blank disk using an external servo writer, by sweeping the servo writer head at a constant speed from the outer to the inner edges of a rotating disk, and will be applied as references to write the final product servos via in-drive self servo writing (SSW) (Sado et al. (2008)).

By the nature of the two stage servo writing process, position errors in the spiral writing process will be transmitted to external disturbances when writing the product servos. Ultra precision is therefore required in the spiral writing stage. As a result, the design of high performance controllers is a key to achieve high quality spiral writing. Most of the current industry

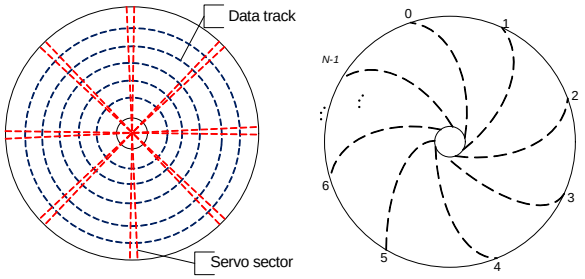

(a) data tracks and servo sectors (b) spiral servo patterns

Fig. 1. Servo patterns on the disk.

patents (Mizukoshi et al. (2010); Vinay K. Agarwal (2006); Kim et al. (2008); Sado et al. (2008)) focus on description of the system and the spiral writing method. Yet, little results on the involved control problem have been published in the open literature. This paper discusses the control design in spiral writing. A new perspective on feedforward design in two degree of freedom (2DOF) control structures will be introduced. The main result from the control algorithm perspective is that, a new robust tracking algorithm is proposed, based on iterative learning control, to generate an asymptotic optimal feedforward control signal. This iterative process can be applied offline first as a training stage. When performing online tracking control, robustness will be added by performing least square estimation at the intervals of each spirals.

The remainder of the paper is organized as follows. Section 2 introduces the spiral writing process and formulates the control problem. In Section 3, the baseline feedback system will be designed. A disturbance observer will be introduced to ensure the availability of an accurate closed loop system structure for the model based feedforward design. An initial feedforward signal will also be designed, using the Zero Phase Error Tracking algorithm (Tomizuka (1987)). Further improving the initial

⋆ This work was supported by the Computer Mechanics Laboratory (CML) in the Department of Mechanical Engineering, University of California at Berkeley.

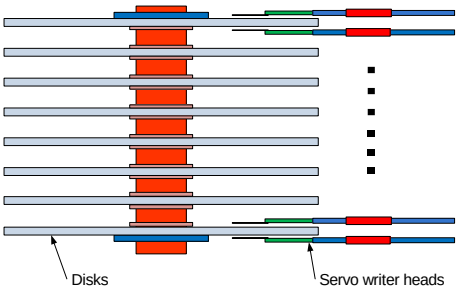

Fig. 2. Demonstration of media servo writing.

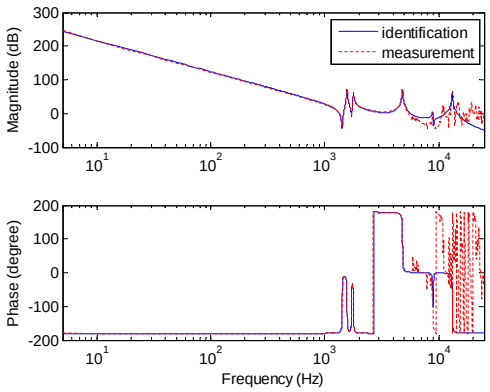

Fig. 3. Frequency response of the servo writing system.

feedforward design, Section 4 develops the new iterative way of updating the feedforward signal to achieve monotonic tracking error decrease. Section 5 discusses methods to reduce the influence of non-repetitive errors during online iterative learning. Section 6 concludes the paper.

2. FORMULATION OF THE CONTROL PROBLEM

Spiral servo writing is performed in a clean environment on media servo writers (Uematsu and Fukushi (2001); Zhu et al. (2005)). To reduce the production time and the usage of clean room space, spirals on multiple disks are written at the same time, using a group of servo writer heads powered by voice coil motors (VCMs), as shown in Fig. 2 (for demonstration, only four heads are sketched). The group of write heads are designed such that they share very similar dynamic characteristics, and small dynamic variations appear only in very high frequency regions. The central head plus its actuator system in Fig. 2 can thus be chosen as the plant for controller design. Figure 3 presents the frequency response of the plant from an actual servo writer system, which can be modeled as the summation of a double integrator plus some vibration modes.

When writing the spirals, the servo writer head moves back and forth between the disk outer diameter (OD) and the inner diameter (ID), laying down the coded magnetic patterns. Figure 4 demonstrates an example of writing eight spirals on a disk, where some so-called seed tracks have been pre-written in OD and ID, and the numbers O1 to O8 indicate the starting positions for the spirals. When writing the first spiral, the head initializes at position O1 and finishes writing at the seed track in ID. After a short settling period, the head returns to its initial position at the OD seed track, and waits for the writing position of the next spiral. Figure 5 presents the reference trajectory used in this

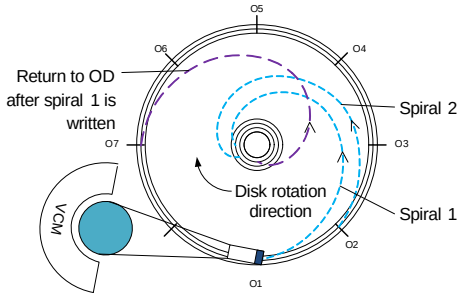

Fig. 4. Spiral writing on a disk platter.

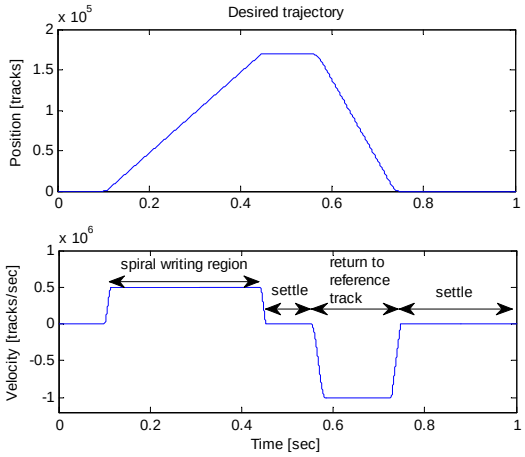

Fig. 5. Reference trajectory for writing one spiral.

paper [1] . The reference profile was designed using the Structural Vibration Minimized Acceleration Trajectory (SMART) (Mizoshita et al. (1996)), to achieve fast acceleration with small excitation of the system vibration modes. After reaching the desired spiral writing speed, the write heads maintain the constant velocity and print down the servo patterns on the disk. When the heads move from ID to OD, spirals are not written, due to the inverse of the velocity direction in Fig. 4. The motion control was thus designed more aggressively, applying greater speed, acceleration and deceleration. A large amount of (usually hundreds of) spirals need to be written in reality. The trajectory in Fig. 5 thus needs to be repeated for many times.

The typical spiral writing speed is between 2 and 6 inches per second. Assume that we are performing spiral writing to 3.5-inch disks. The process parameters used in this paper are summarized as follows:

$$\begin{aligned} \text{Spiral writing speed} &: 5 \text{ inch/sec} \\ \text{Maximum acceleration of the writer head} &: 500 \text{ inch}/\text{sec}^2 \\ \text{Sector number per track} &: 220 \\ \text{Track density} &: 100 \text{ kTPI} \\ \text{Track pitch} &: 25.4 \text{ nm} \end{aligned} \tag{1}$$

Notice that for the servo write head, the initial position to write each spiral is the same. The control problem can thus be summarized as: given a reference trajectory in Fig. 5, perform fast and accurate tracking control for multiple times, with the same start position for the servo write head at each repetition.

[1] The position has been normalized w.r.t. the center of the OD seed track.

3. BASELINE TWO DEGREE OF FREEDOM CONTROL

The writing of spirals is a typical tracking control problem. This section provides a two degree of freedom controller structure for spiral writing. This structure will be applied as a baseline for the iterative learning design in the next section, to develop an asymptotically optimal feedforward input. The proposed 2DOF structure is shown in Fig. 6, where $G_p\left(z^{-1}\right)$ and $z^{-m}G_n(z^{-1})$ are respectively the discretized full-order plant and its low-order nominal model (m denotes the relative degree of the nominal model); $G_{notch}\left(z^{-1}\right)$ is a group of notch filters to attenuate the plant resonance modes; $G_{PD}\left(z^{-1}\right)$ is a feedback proportional–derivative (PD) controller [2] ; and $Q(z^{-1})$ is a low-pass filter. The output $y(k)$ is the position of the servo writer head in the unit of track pitch (TP). $y_d(k)$ is the reference trajectory which $y(k)$ is expected to follow with high accuracy. The system is subjected to input and output disturbances, denoted as $w(k)$ and $d(k)$.

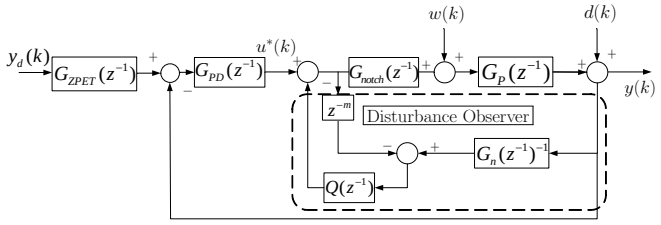

Fig. 6. Proposed controller structure for single spiral writing.

The delay z^{-m}, the inverse of the nominal model, and the Q-filter $Q\left(z^{-1}\right)$, form the so-called disturbance observer (DOB), which has been effectively applied to various types of motion control systems (see, for example, Yang et al. (2005); White et al. (2000); Tan et al. (2003)). If one cuts the main feedback loop at the output of $G_{PD}\left(z^{-1}\right)$, and analyze the inner loop formed by the plant, the notch filter $G_{notch}\left(z^{-1}\right)$, and the DOB, one can find that the transfer function between $u^*(k)$ and $y(k)$ is given by

$$G_{u^*y}\left(z^{-1}\right)=\frac{\bar{G}_p\left(z^{-1}\right)G_n\left(z^{-1}\right)}{G_n\left(z^{-1}\right)+\left[\bar{G}_p\left(z^{-1}\right)-z^{-m}G_n\left(z^{-1}\right)\right]Q\left(z^{-1}\right)},$$

where $\bar{G}_p\left(z^{-1}\right)=G_p\left(z^{-1}\right)G_{notch}\left(z^{-1}\right)$.

In the low frequency region where $Q(z^{-1})\approx 1$, when the delay step m is small such that $(1-z^{-m})G_n\left(z^{-1}\right)\approx 0$, we have $G_{u^*y}\left(z^{-1}\right)\approx G_n\left(z^{-1}\right)$ in the above equation. The entire DOB loop thus behaves like the nominal plant $G_n(z^{-1})$. Therefore, in the low frequency region where tracking control is performed, the plant uncertainty is greatly attenuated and high performance model based feedforward design can be achieved. In the high frequency region where $Q\left(z^{-1}\right)\approx 0$, the DOB loop is essentially cut off, and $G_{u^*y}\left(z^{-1}\right)$ is nothing but $\bar{G}_p\left(z^{-1}\right)$, i.e., the original plant cascaded with the notch filters. Applying similar analysis to the transfer functions between the disturbances and the output, one can find that DOB also compensates the low-frequency input and output disturbances.

The disturbance observer makes the DOB loop behave like the nominal plant $G_n(z^{-1})$, and remain robust in the presence of low frequency disturbances. Therefore, below the cut-off frequency of $Q(z^{-1})$ (for discussions on the design of $Q\left(z^{-1}\right)$, see for example, Choi et al. (2003) and Chen and Tomizuka (2010)), the closed loop transfer function will be close to

$$G_{closed}(z^{-1})=\frac{G_n(z^{-1})G_{PD}(z^{-1})}{1+G_n(z^{-1})G_{PD}(z^{-1})}. \tag{2}$$

Based on $G_{closed}(z^{-1})$, high performance feed-forward controllers can now be designed. One effective method is to apply the Zero Phase Error Tracking (ZPET) algorithm (Tomizuka (1987)), where the overall transfer function of the feedback loop is partitioned by

$$G_{closed}(z^{-1})=\frac{z^{-d}B_c(z^{-1})}{A_c(z^{-1})}=\frac{z^{-d}B_c^-(z^{-1})B_c^+(z^{-1})}{A_c(z^{-1})}. \tag{3}$$

In (3), $B_c^-(z^{-1})$, $B_c^+(z^{-1})$ and $A_c(z^{-1})$ denote respectively the unstable (or more generally, non-cancellable) numerator part, the cancellable numerator part, and the stable closed loop characteristic polynomial. The ZPET controller cancels the cancellable poles and zeros in $G_{closed}(z^{-1})$, and introduces some additional terms as follows:

$$G_{ZPET}(z^{-1})=z^d\frac{A_c(z^{-1})B_c^-(z)}{B_c^+(z^{-1})B_c^-(1)^2}, \tag{4}$$

where $B_c^-(z)$ is derived by replacing every z^{-1} in $B_c^-(z^{-1})$ with z, and $B_c^-(1)$ is obtained through replacing every z^{-1} in $B_c^-(z^{-1})$ with 1.

The overall transfer function from $y_d(k)$ to $y(k)$ is therefore given by

$$G_{all}(z^{-1})=G_{ZPET}(z^{-1})G_{closed}(z^{-1})=\frac{B_c^-(z^{-1})B_c^-(z)}{B_c^-(1)^2}. \tag{5}$$

In the spiral writing case, $G_{closed}\left(z^{-1}\right)$ has one uncancellable zero at $z=-1$, due to the double integrator type low frequency dynamics in the plant. We thus have

$$G_{all}=\frac{(1+z^{-1})(1+z)}{4}, \tag{6}$$

which is a zero-phase low-pass filter. It has been shown in Tomizuka (1987) that if the desired position trajectory is either a step or a ramp signal, the above ZPET control algorithm achieves asymptotic perfect tracking.

The transfer function in (4) is not directly implementable. Denoting s as the order of $B_c^-(z)$, we instead add $d+s$ steps of delays to (4) and apply the $d+s$ step-advanced version of the reference trajectory as the new reference input.

4. OFFLINE OPTIMAL FEEDFORWARD DESIGN

Summarizing the results in the last section, we have designed the feedback system such that a closed loop model $G_{closed}\left(z^{-1}\right)$ is relatively accurate below the cut-off frequency of $Q\left(z^{-1}\right)$. We have designed a feedforward signal, denoted as $\tilde{u}(k)$ in Fig. 7, that is applied as the input to the closed loop system. Essentially, the control aim is to design $\tilde{u}(k)$ so that $y(k)$ tracks $y_d(k)$ as closely as possible. In the traditional 2DOF system design, $\tilde{u}(k)$ is designed based on only the desired reference $y_d(k)$, as is the case in the ZPET design in Section 3. In this section, based on the achieved results in the last section, a new design of $\tilde{u}(k)$ is presented, which combines the usage of $y_d(k)$ and $y(k)$, i.e., using some extra "feedback" (in a new iteration domain) of the tracking result. The key foundation of the

[2] A PD controller is used here instead of a more general PID controller, since the disturbance observer to be introduced provides the integral action already.

following design is the fact that the DOB inside the closed loop system has lead to a relatively accurate $G_{closed}\left(z^{-1}\right)$ (at least in the desired region for tracking control), and the algorithm we derive is generated from the idea in iterative learning control.

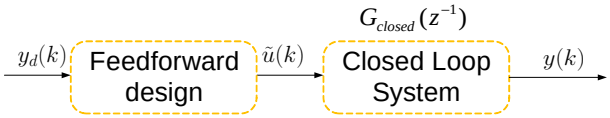

Fig. 7. Summary of the feedforward design in Section 3.

Suppose we have finished the simulation/experiment using the control structure in Fig. 6. The tracking error $e_1(k) = y_d(k) - y(k)$ is calculated to analyze the tracking performance. To improve the feedforward input, we wish to incorporate the tracking error $e_1(k)$. Consider running the overall system for a second time, but with an additional feedforward input $u_2(k)$ (here the subscript indicates the iteration number). This is shown in Fig. 8, where the dotted lines indicate the process of collecting the previously obtained information.

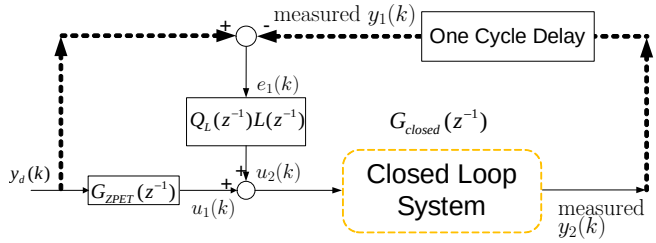

Fig. 8. Block diagram of learning control at iteration 2.

In Fig. 8, $L(z^{-1})$ is a learning filter and $Q_L\left(z^{-1}\right)$ is a zero-phase low-pass filter to improve the system robustness. The learning process can be repeated, to form Fig. 9. We observe that, if the closed loop system does not change much at frequencies where accurate tracking is required, errors in the previous processes may be effectively used to produce an improved feedforward signal $u_j(k)$ at the j^{th} iteration. The requirement on the closed loop system is addressed by the DOB designed in the last section, which assures that below the cut-off frequency of the Q-filter, the closed loop system is close to the nominal transfer function $G_{closed}\left(z^{-1}\right)$ in (2). We now focus on the design of $L\left(z^{-1}\right)$ and $Q_L\left(z^{-1}\right)$.

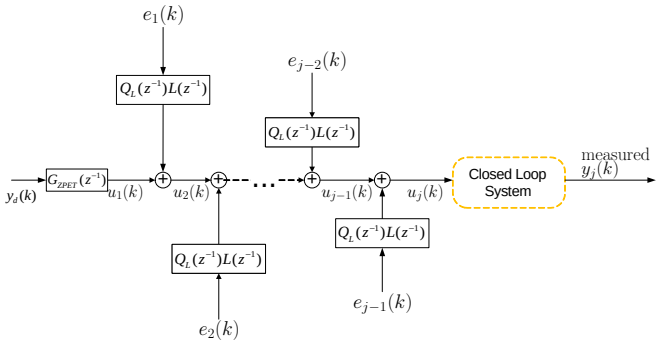

Fig. 9. Tracking control via learning from all previous errors.

4.1 Design of the Learning Process

The block diagram in Fig. 9 can be equivalently represented by that in Fig. 10. As mentioned in Section 2, the servo write heads

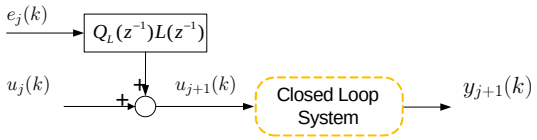

Fig. 10. Simplified form of Fig. 9.

start from the same zero initial condition at each iteration, i.e., $y_j(0) = 0\ \forall j \geq 1$ and $u_j(k) = 0\ \forall k < 0,\ j \geq 1$. For simplicity and consistency with the content in the following section, we denote the transfer function from $u_j(k)$ to $y_j(k)$ as $T_u\left(z^{-1}\right)$, instead of $G_{closed}\left(z^{-1}\right)$ in the previous discussion.

We consider first the case that there is no external disturbances to the system. This disturbance free condition will be dropped in the next section, where a robust learning algorithm is provided. The input-output relation in Fig. 10 is given by

$$y_{j+1}(k) = T_u\left(z^{-1}\right) u_{j+1}(k). \tag{7}$$

At the j^{th} iteration, the tracking error is given by $e_j(k) = y_d(k) - y_j(k)$. Applying the learning control in Fig. 10 yields

$$u_{j+1}(k) = u_j(k) + Q_L\left(z^{-1}\right) L\left(z^{-1}\right) e_j(k). \tag{8}$$

Notice that different from traditional iterative learning control, where $u_{j+1}(k) = Q_L\left(z^{-1}\right)\left(u_j(k) + L\left(z^{-1}\right) e_j(k)\right)$, the filter $Q_L\left(z^{-1}\right)$ is applied directly to $L\left(z^{-1}\right) e_j(k)$ in (8). This occurs since at the initial iteration, the feedforward input $u_1(k)$ developed in Section 3 already achieves low-pass type overall dynamics from $y_d(k)$ to $y(k)$. Applying additional low-pass filtering to $u_1(k)$ thus will not necessarily improve the tracking performance. By the same reasoning, $u_j(k)$ does not need to be processed by $Q_L\left(z^{-1}\right)$, if the learning scheme is well designed.

To obtain a relationship between the tracking errors, we first notice that $e_{j+1}(k)$ is given by $e_{j+1}(k) = y_d(k) - y_{j+1}(k)$. Substituting (7) and (8) to this relation yields

$$\begin{aligned} e_{j+1}(k) = y_d(k) - T_u\left(z^{-1}\right) u_j(k) \\ - \left[T_u\left(z^{-1}\right) Q_L\left(z^{-1}\right) L\left(z^{-1}\right)\right] e_j(k). \end{aligned} \tag{9}$$

Notice that $T_u\left(z^{-1}\right) u_j(k)$ is nothing but $y_j(k)$, and that $y_d(k) - y_j(k) = e_j(k)$. Equation (9) thus becomes

$$e_{j+1}(k) = \left[1 - T_u\left(z^{-1}\right) Q_L\left(z^{-1}\right) L\left(z^{-1}\right)\right] e_j(k). \tag{10}$$

The ideal error learning would thus occur if $L\left(z^{-1}\right) = T_u^{-1}\left(z^{-1}\right)$ and $Q_L\left(z^{-1}\right) = 1$. In that case, the maximum convergence rate is achieved, and the error goes to zero in one iteration. Unfortunately, this can hardly be realized in practice since the exact stable inverse is usually unavailable. Yet, recalling the design of the ZPET controller in Section 3, $G_{ZPET}\left(z^{-1}\right)$ is nothing but an approximation of the inverse of $T_u\left(z^{-1}\right) = G_{closed}\left(z^{-1}\right)$. Therefore, it makes sense to use $G_{ZPET}\left(z^{-1}\right)$ as a learning filter.

4.2 Analysis of Stability

Applying the results in the last subsection, and recalling (5) and (6), we have, in the spiral writing process,

$$L\left(z^{-1}\right) T_u\left(z^{-1}\right) = G_{ZPET}(z^{-1}) G_{closed}(z^{-1}) \tag{11}$$

$$= \frac{B_c^-(z^{-1}) B_c^-(z)}{B_c^-(1)^2} = \frac{(1+z^{-1})(1+z)}{4}. \tag{12}$$

The above transfer function is a zero-phase low-pass filter whose magnitude is always less than or equal to 1. The low-pass filter $Q_L\left(z^{-1}\right)$ in (10) is also zero-phase. Therefore $1-L(z^{-1})Q_L\left(z^{-1}\right)T_u(z^{-1})$ in (10) satisfies

$$|1-L\left(e^{-j\omega}\right)Q_L\left(e^{-j\omega}\right)T_u\left(e^{-j\omega}\right)|<1,\ \forall\omega>0. \qquad (13)$$

Notice that (10) describes a dynamic system in the iteration domain. Equation (13) therefore indicates that the proposed learning structure is asymptotically stable. The tracking error reduces monotonically at each iteration, and the feedforward input sequence asymptotically drives $e_j(k)$ to zero.

4.3 Design of Zero Phase Low-pass Filters

Different methods exist for designing zero phase filters. One way is to use the command *filtfilt* in MATLAB, which performs a time inverse to the data, and applies a non-zero-phase filter twice. An alternative design in the transfer function domain is proposed as follows:

$$Q_L\left(z^{-1}\right)=\frac{(1+z^{-1})(1+z)}{4}\cdot\prod_{i=0}^{M}\left(\frac{1-2\beta_i z^{-1}+z^{-2}}{2-2\beta_i}\cdot\frac{1-2\beta_i z+z^2}{2-2\beta_i}\right). \qquad (14)$$

The first part of the right hand side of (14) is a zero-phase low-pass filter with two zeros at $z=-1$, as has been shown before. In the second part, β_i is proposed to be chosen by $\beta_i=\cos(2\pi\Omega_i T_s)=\left(e^{j2\pi\Omega_i T_s}+e^{-j2\pi\Omega_i T_s}\right)/2$, resulting in $1-2\beta_i z^{-1}+z^{-2}$ to have two zeros $e^{\pm j2\pi\Omega_i T_s}$ (T_s denotes the sampling frequency) on the unit circle at the frequency Ω_i (in Hz). By such a construction, one can tune the bandwidth of the low-pass filter, and in addition avoids the learning of the non-repeatable disturbances whose energy is highly concentrated at Ω_i. In the remaining components of (14), $1-2\beta_i z+z^2$ is the complex conjugate of $1-2\beta_i z^{-1}+z^{-2}$, resulting in the zero phase property of $\left(1-2\beta_i z+z^2\right)\left(1-2\beta_i z^{-1}+z^{-2}\right)$. Finally, $2-2\beta_i$ normalizes the DC gain to one, and M is the number of zero-phase blocks that the designer chooses. Figure 11 shows the magnitude response of an example of $Q_L\left(z^{-1}\right)$, where $M=2$, $\beta_1=\cos(2\pi T_s\times 7880)$, $\beta_2=\cos(2\pi T_s\times 9858)$, and $T_s=1/26400$ sec. Such a $Q_L\left(z^{-1}\right)$, if used in (8), will filter out the high frequency parts in $e_j(k)$ and enforce strong attenuation of the error components at 7880 Hz and 9858 Hz.

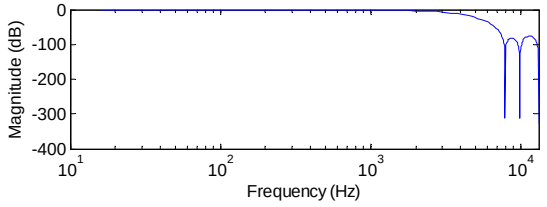

Fig. 11. Magnitude response of a $Q_L\left(z^{-1}\right)$ designed from (14).

4.4 Offline Learning Results

We now implement the proposed algorithm to the spiral writing process. Multiple iterations are applied offline in simulation, to train the feedforward signal. $Q_L\left(z^{-1}\right)$ in (14) was designed with $M=0$, i.e., no priori information of the tracking error spectrum is assumed. Figure 12 shows the stacked time trace of the tracking errors over fourteen iterations. Each iteration lasts one second. Referring to the trajectory profile in Fig. 5, we see that in Fig. 12, large errors occurred at the transitions between different spiral writing stages (around 0.1 sec, 0.44 sec, 0.57 sec, and 0.75 sec in Fig. 5); while at the constant spiral writing region, the steady state tracking error is 0 due to the ZPET design in Section 3.

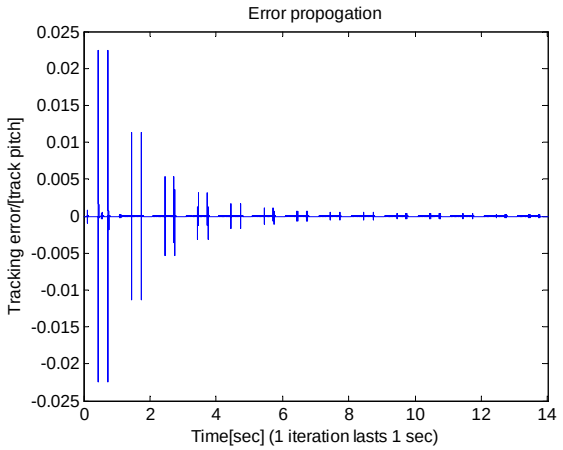

Fig. 12. Simulated tracking errors in the offline learning.

For the iterative learning performance, it is observed that although the maximum value of the error in the initial iteration was already quite small (less than 0.02 track pitch (TP); 1 TP = 254 nm), after four iterations, more than eighty percent reduction was achieved in the maximum error magnitudes. In Fig. 13, stability and convergence of the learning process are graphically shown from the propagation of the l_2 norm of the tracking errors. With the offline learned results, a feedforward signal is generated, that asymptotically drives the tracking error to zero. After sufficient learning, e.g., 10 iterations of simulations (maximum tracking error less than 0.05% track pitch), the feedforward input at the end of iteration 10 can be collected and stored as a vector, to be applied for real time implementation.

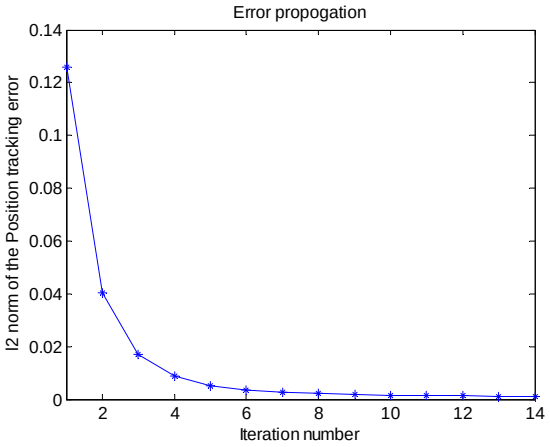

Fig. 13. l_2 norm of the tracking errors in Fig. 12.

5. ONLINE ROBUST ITERATIVE LEARNING CONTROL

The proposed offline learning scheme in the last section is optimal in the sense of trajectory tracking, i.e., without the influence of external disturbances. In spiral writing, the repetitive nature

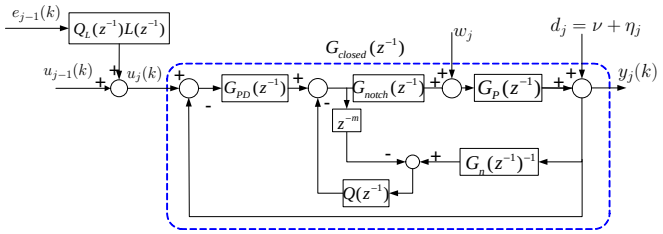

Fig. 14. Block diagram for spiral writing with iterative learning.

of the process generates iteration independent disturbances. Additionally, non-repeatable disturbances, such as measurement noise, environment changes, etc, also exist. In this section, the learning scheme in the last section is extended to online processes, to reduce also the iteration independent disturbance, without amplification of the non-repeatable ones. Figure 14 demonstrates the general block diagram that combines Fig. 6 and Fig. 10, where we have lumped the iteration independent disturbance ν at the plant output side, and introduced subscripts to the non-repeatable disturbances w_j and η_j to indicate their dependence on the iteration number j. The disturbance profile we employ in this section is obtained from a realistic benchmark HDD problem developed by a technical committee of IEE Japan (IEEJ, Technical Commitee for Novel Nanoscale Servo Control (2007)). Servo track writers are much more precise machines than HDDs. Our simulation can therefore be regarded as a worst case analysis of what may happen in actual servo track writing.

To analyze the effects of the various disturbances, we denote the transfer functions from $w_j(k)$ to $y_j(k)$ and from $d_j(k)$ to $y_j(k)$, as $T_w\left(z^{-1}\right)$ and $T_d\left(z^{-1}\right)$ respectively. The input-output relation is then given by [3]

$$y_{j+1} = T_u u_{j+1} + T_w w_{j+1} + T_d\left(\nu + \eta_{j+1}\right). \tag{15}$$

Applying similar error dynamics analysis as that in Section 4, we can obtain the tracking error

$$\begin{aligned} e_{j+1} &= y_d - y_{j+1} \\ &= y_d - T_u u_{j+1} - T_w w_{j+1} - T_d\left(\nu + \eta_{j+1}\right). \end{aligned} \tag{16}$$

Intuitively, e_j also contains rich information about the repeatable tracking error ν. If we use the same learning law as that in (8), i.e., $u_{j+1} = u_j + (Q_L L)\, e_j$, (16) becomes

$$\begin{aligned} e_{j+1} = y_d - T_u u_j - (T_u Q_L L)\, e_j \\ - T_w w_{j+1} - T_d\left(\nu + \eta_{j+1}\right). \end{aligned} \tag{17}$$

From (15), we have $y_j = T_u u_j + T_w w_j + T_d(\nu + \eta_j)$. Solving for $T_u u_j$ from this equation and substituting the result to (17) yields

$$\begin{aligned} e_{j+1} = y_d - y_j - (T_u Q_L L)\, e_j + T_w w_j + T_d(\nu + \eta_j) \\ - \left[T_w w_{j+1} + T_d\left(\nu + \eta_{j+1}\right)\right]. \end{aligned} \tag{18}$$

Noticing that the first two terms on the right hand side of (18) equals to e_j, we get

$$\begin{aligned} e_{j+1} = (1 - T_u Q_L L)\, e_j + T_d(\nu - \nu) \\ + T_w\left(w_j - w_{j+1}\right) + T_d\left(\eta_j - \eta_{j+1}\right). \end{aligned} \tag{19}$$

We observe from the above error dynamics, that: (1), the second term on the right hand side of the equation is 0 regardless of T_d, i.e., the repetitive disturbance ν is rejected; (2), the propagation of the non-repeatable errors depends on the closed loop transfer functions T_w and T_d, which are independent of the feedforward design [4]. The last term that introduces learning errors in (19) is e_j. To achieve a learning algorithm that is robust also in the non-repeatable disturbances, we consider e_j from a different view point, by partitioning (16) and changing the iteration index, to obtain

$$e_j = y_d - T_u u_j - T_w w_j - T_d(\nu + \eta_j), \tag{20}$$

$$= \underbrace{(y_d - T_u u_j - T_d \nu)}_{\text{repeatable error } \varepsilon_j} - \underbrace{(T_w w_j + T_d \eta_j)}_{\text{nonrepeatable error } \bar{n}_j} \tag{21}$$

where $\varepsilon_j(k)$ is the tracking error when the system is subjected only to the repetitive output disturbance ν, and is the real signal that needs to be learned.

To extract ε_j from e_j, we apply the least mean square error estimation to minimize the following cost function:

$$J_{j,k} = E\left[\sum_{k=0}^{N}\left(\varepsilon_j(k) - \hat{\varepsilon}_j(k)\right)^2\right], \tag{22}$$

where N is the sample length of one iteration. The expectation and the summation operations can be interchanged. We then have

$$J_{j,k} = \sum_{k=0}^{N}\left\{E\left(\varepsilon_j^2(k)\right) + \hat{\varepsilon}_j^2(k) - 2\hat{\varepsilon}_j(k)\, E\left(\varepsilon_j(k)\right)\right\},$$

which is a convex function of the decision variable $\hat{\varepsilon}_j(k)$. Taking the first derivative of $J_{j,k}$ w.r.t. $\hat{\varepsilon}_j(k)$, and set the result to zero, one can obtain that $J_{j,k}$ achieves its minimum at

$$\hat{\varepsilon}_j(k) = E\left[\varepsilon_j(k)\right] = E\left[e_j(k) + \bar{n}_j\right] = E\left[e_j(k)\right], \tag{23}$$

where we have substituted in (21) and assumed that the non-repeatable error $\bar{n}_j$ has zero mean. The expectation can only be approximated from the empirical mean. We thus get the realizable best estimation of the repeatable error

$$\hat{\varepsilon}_j(k) = \frac{1}{j}\sum_{i=1}^{j-1} e_i(k) \tag{24}$$

The learning control law is then modified to be

$$u_{j+1}(k) = u_j(k) + Q_L\left(z^{-1}\right) L\left(z^{-1}\right) \hat{\varepsilon}_{j+1}(k) \tag{25}$$

The above robust learning algorithm was implemented in spiral servo writing. 56 spirals were written, with the HDD disturbance profile discussed at the beginning of this section. The results are shown in Fig. 16. The online learning using the normal learning algorithm in Section 4 was also performed, as shown in Fig. 15. In both cases, we have applied the same $Q_L\left(z^{-1}\right)$ given by Fig. 11. It is observed that: (a), normal iterative learning did not improve the tracking performance, due to the presence of various non-repeatable disturbances; (b), compared with the results in the normal learning case, using the proposed robust learning scheme, after a transient response of two iterations, the norms of the tracking errors follow a decreasing trend. The l_2 norm decreased from 5.27 to about 4.4 at the end of iteration 56, which is close to the result (4.1814) when we apply no external repetitive disturbances. This indicates that we have effectively attenuated the repeatable error $\varepsilon(k)$ using the proposed algorithm.

[3] To simplify the notations, we drop the time index k and the z-domain index z when no confusion is generated.

[4] Yet, $T_w\left(w_j - w_{j+1}\right)$ may be small if w_j and w_{j+1} are close to each other, i.e., the low frequency non-repeatable disturbances can get attenuated.

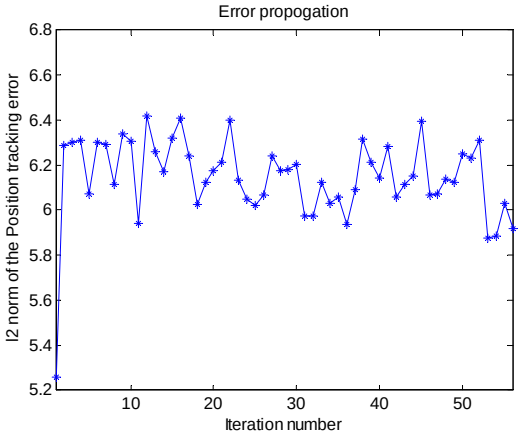

Fig. 15. l_2 norm of the simulated tracking errors using normal iterative learning control.

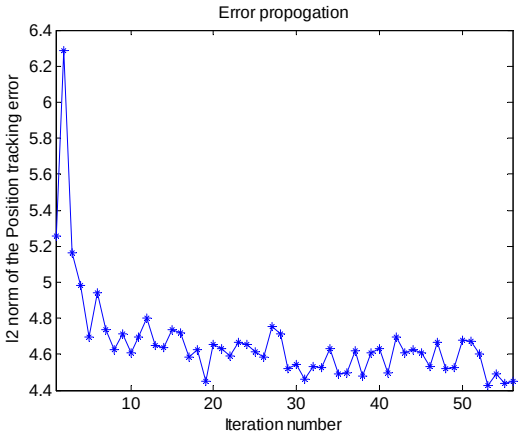

Fig. 16. l_2 norm of the simulated tracking errors using the proposed robust iterative learning control.

6. CONCLUSIONS AND FUTURE RESEARCH

In this paper, the position control problem in spiral servo writing has been discussed. An iterative learning control scheme has been developed and a new method of designing feedforward control inputs has been proposed. Performance of the proposed controllers was verified in both deterministic and noisy environments. The simulation results agree with the predicted system behavior. The proposed method is expected to be effective in other problems that require learning of feedforward control input in the presence of repetitive and non-repetitive disturbances.

Future research includes improving the stochastic behavior in Section 5. The filtering process is essentially conducting signal processing in a new iteration domain. Enhancement may be achieved if a more proper cost function or additional constraints are applied.

REFERENCES

Al Mamun, A., Guo, G., and Bi, C. (2007). *Hard disk drive: mechatronics and control*. CRC Press.

Chen, X. and Tomizuka, M. (2010). Optimal plant shaping for high bandwidth disturbance rejection in discrete disturbance observers. In *Proceedings of the 2010 American Control Conference, Jun. 30-Jul. 02, 2010, Baltimore, Maryland*, 2641–2646.

Choi, Y., Yang, K., Chung, W., Kim, H., and Suh, I. (2003). On the robustness and performance of disturbance observers for second-order systems. *IEEE Transactions on Automatic Control*, 48(2), 315–320.

IEEJ, Technical Commitee for Novel Nanoscale Servo Control (2007). NSS benchmark problem of hard disk drive systems. http://mizugaki.iis.u-tokyo.ac.jp/nss/.

Kim, C., Shim, J., and Park, S. (2008). Method for writing spiral reference servo signal in hard disk drive and method for compensating for temperature, US Patent 7321479.

Mizoshita, Y., Hasegawa, S., and Takaishi, K. (1996). Vibration minimized access control for disk drives. *IEEE Transactions on Magnetics*, 32(3 Part 2), 1793–1798.

Mizukoshi, S., Yatsu, M., Sado, H., Ueda, K., Matsunaga, T., Kouhara, S., Nakajima, S., et al. (2010). Method and apparatus for writing spiral servo pattern in a disk drive, US Patent 7710682.

Sado, H., Yatsu, M., Ueda, K., Matsunaga, T., Mizukoshi, S., Nakajima, S., and Kouhara, S. (2008). Method and apparatus for writing servo data in a disk drive using spiral servo patterns, US Patent 7477472.

Tan, K., Lee, T., Dou, H., Chin, S., and Zhao, S. (2003). Precision motion control with disturbance observer for pulsewidth-modulated-driven permanent-magnet linear motors. *IEEE Transactions on Magnetics*, 39(3 Part 2), 1813–1818.

Tomizuka, M. (1987). Zero phase error tracking algorithm for digital control. *Journal of Dynamic Systems, Measurement, and Control*, 109(1), 65–68.

Uematsu, Y. and Fukushi, M. (2001). Servo track writing technology. *Fujitsu Scientific and Technical Journal*, 37(2), 220–226.

Vinay K. Agarwal, R.L.C. (2006). Using an external spiral servo writer to write spiral reference patterns to a disk to facilitate writing product servo bursts to the disk, US Patent 6992848.

White, M., Tomizuka, M., and Smith, C. (2000). Improved track following in magnetic disk drives using a disturbance observer. *IEEE/ASME Transactions on Mechatronics*, 5(1), 3–11.

Yang, K., Choi, Y., and Chung, W.K. (2005). On the tracking performance improvement of optical disk drive servo systems using error-based disturbance observer. *IEEE Transactions on Industrial Electronics*, 52(1), 270–279.

Zhu, J., Moraru, A., Zanetti, T., Tao, F., Kilmer, D., Hess, H., Carr, T., Bellis, M., Pinto, G., and Lee, P. (2005). Media servowriting system, US Patent 6977791.